

BLEED PERTURBATION ACTIVE CONTROL OF FOREBODY ASYMMETRIC VORTICES

Xueying Deng, Xuerui Chen and Yankui Wang
Beijing University of Aeronautics and Astronautics

Keywords: asymmetric vortex, active control, high angle of attack aerodynamics, slender body

Abstract

The effects of nose perturbations on the behaviors of asymmetric vortices over a slender body have been studied. The tests have been conducted at low speed wind tunnel with subcritical Reynolds number of 1×10^5 at angle of attack $\alpha = 50^\circ$. The experiments results show that there are four sensitive circumferential locations of manual perturbation at which bistable vortices over slender body are switched by the perturbation. And if the rate of microblowing at nose tip as a perturbation is increased a new flow phenomena has been found in which the two-cycle behavior of C_y vs. γ curve is gradually evolved into one-cycle. Based on that phenomenon, a new asymmetric vortex control technique that is called bleed perturbation active control is developed. This control technique not only can change the vortices positions between a yaw-left and yaw-right configuration to change the sign of side force but also can make the magnitude of side force to be variable even at bistable state of asymmetric vortex.

1 Introduction

In order to improve the agility and maneuverability of the advance fighter aircraft in the air combat, it would operate at high angles of attack for maximum lift and in the post stall regime. However the conventional control surfaces, such as the vertical tail and rudder, become ineffective at high angle of attack when they are immersed in the low energy separated flow from the wing and fuselage. On the other hand, the well-known vortex asymmetry occurring on pointed

forebody at high angles of attack, which generate the side force acting on the forebody. With increasing in angles of attack, the rudder effectiveness is decreasing, the asymmetry vortices are developed and side force of the forebody vortices is increasing. If the forebody asymmetric vortices can be controlled, then they can be used for generating a controlled yawing moment to replace the lost yaw controllability from the rudder. Therefore the subject of forebody vortex control has received much attention and extensive research studies have been carried out^[1-9]. During the studies, it is highly desirable to have forebody vortex control devices that not only are simple in design but also have no complex additional parts. From present knowledge^[10-13], the asymmetry vortices system over pointed forebody is very sensitive to the disturbance on or near the nose tip. Therefore active forebody vortex control techniques with nose micro-disturbance have investigated intensively^[2,3,6-9,14,15]. In some techniques the microblowing or unsteady bleed as a nose disturbance are used to manipulate the development of forebody asymmetric vortices. In the experimental studies by Roos^[14] and Williams^[4], the control ports consisted of two small holes on each side of nose tip and located at $\pm 135^\circ$ from the windward meridian of the forebody. However their experimental results show that if angle of attack is high enough, such as $\alpha = 50^\circ$, the asymmetric vortices over slender body with pointed nose appear the behavior of bistable state and the available results of asymmetric vortices control with unsteady bleed or microblowing show so far that the behavior of asymmetric vortices is too sensitive to blowing perturbation and the blowing-effectiveness C_y vs. C_μ appears jump characteristics corresponding to the bistable

state behavior of asymmetric vortices, where C_y is side force coefficient and C_μ is blowing momentum coefficient. Therefore it is difficult to apply it into control technique.

In order to improve this control characteristics the present study has found a new flow phenomena with microblowing at nose tip as a perturbation to the asymmetric vortices flow, based on which a new vortex control technique that is called bleed perturbation active control is developed. This control technique not only can change the vortices positions between a yaw-left and yaw-right configuration to change the sign of side force but also can make the magnitude of side force to be variable.

2 Wind Tunnel, Model and Test Conditions

Two wind tunnel testing pressure tapped models are designed as shown in Fig.1. Both of noses were pointed tangent ogives of fineness ratio 3 with same contour. A piece of manual micro-triangle block as perturbation is added on nose of model I as shown in Fig.1a). One bleed orifice with diameter 0.5mm is drilled on the nose tip of the model II as shown in Fig.1b). The afterbody of model I and II are circular cylinder.

The pressure tapped model I was tested in NF-3 wind tunnel in Northwest Polytechnical University with test section 3m×1.6m. The freestream turbulence level in NF-3 is approximately 0.045%. The second model II was tested in D-4 Low Speed Tunnel in Beijing University of Aeronautics and Astronautics with test section 1.5m×1.5m and its turbulence level is 0.085%.

The tests of pressure measurement were carried out in both wind tunnels of NF-3 and D-4 Low Speed Tunnel with same Reynolds number $Re_D = V_\infty D / \nu = 1.0 \times 10^5$, where D is diameter of the model afterbody.

The pressure measurement systems are PSI 8400 electronic scanivalve and Scanivalve mechanical pressure scanivalve system with pressure transducers accuracy of 0.05% in NF-3 and D-4 LST respectively.

3 Results and Discussions

3.1 Correlation of perturbation circumferential location and asymmetric vortex response

The influence of circumferential location of perturbation on the asymmetric vortices flow can be analyzed with the results of model I tests with roll angle variation. As shown in Fig.2, when the circumferential location of perturbation block is rotated with rotation of the model, the asymmetric vortices flowfield over the model exhibit two alternative switched regular states named as Left Vortex Pattern (LVP) and Right Vortex Pattern (RVP). LVP represents the left vortex (look upstream) of the asymmetric vortices is near to the model surface, while the right vortex is far from the model surface, which results in negative side force. When the model is rotated about its body axis, as shown in Fig.2, at the first it appears RVP at $\gamma = 0^\circ$ then it abruptly switches to LVP when perturbation block is rotated. As the rotation continues, the LVP and RVP switch over alternatively when the azimuthal orientation of perturbation block is at $\theta = 75^\circ, 180^\circ$ and 285° . It can be found that when the micro-perturbation block on the model nose tip is rotated over 360° with model I, the asymmetric vortices flow pattern at bistable state will switch over two cycle. Therefore a close correlation between circumferential position of manual micro-perturbation block and the response of asymmetric vortices flow pattern is revealed.

3.2 Effect of circumferential location of perturbation with small C_μ

Asymmetric vortices flow is very sensitive to the perturbation on nose tip, especially to its circumferential location. Even without bleed, the asymmetric vortices of over the model will be changed with roll angle due to the perturbation of minute irregularities on the nose tip from model machining tolerances. The curves of sectional side force C_y with roll angles γ from model II tests are shown in Fig.3a without bleed. This specific shape of C_y

vs. γ curve is different from one model to another due to different irregularities on the model. These irregularities are called as background perturbation, which depends on the model machining condition. The general feature of curves C_y vs. γ from background perturbation of model appears two-cycle behavior. If a very small bleed $C\mu$ perturbation is added ($C\mu=2 \times 10^{-6}$), the curves C_y vs. γ are still kept the two-cycle behavior as shown in Fig.3b. It is clear shown a typical bistable state behavior of asymmetric vortices from Fig.3. If the circumferential position of perturbation is changed properly the vortices will switch rapidly to the mirror image of original state and the side force appears jump feature.

3.3 Effect of circumferential location of bleed perturbation with variable $C\mu$

From the results of model II testing with variable bleed rate it can be found that if the blowing rate is increased, a new vortices flow phenomena appears which reveals the curve C_y vs. γ to be changed from two-cycle behavior into one-cycle. This flow phenomena can be clearly seen in Fig.3 that the curves C_y vs. γ at sectional station $x/D=3.35$, at which the maximum side force is reached, appear the feature of variation with blowing rate. An important phenomena can be found from Fig.4 that the magnitude of side force coefficient can be made variable gradually from negative value to positive one with blowing rate within a certain range of circumferential bleed position which is called circumferential region of vortex pattern. In the present model experiments, this circumferential regions are $\gamma = 45^\circ \sim 135^\circ$ and $\gamma = 315^\circ \sim 345^\circ$. However it is clear to show in Fig4 that there are other circumferential regions, where vortex patterns and side forces are kept constant with blowing rate, which are called invariable region. From this experiment results, it explain why previous investigators could not obtain a proper control of C_y with bleed technique because their selected bleed circumferential positions located in the invariable regions with blowing rate.

3.4 Control behavior of side force with blowing rate

In order to obtain the proper control behavior of C_y it is very important to select correctly circumferential bleed position from variable region of vortex pattern. The model II testing results of sectional side force C_y vs. $C\mu$ at $x/D=3.35$ under blowing at circumferential position from 60° to 180° are shown in Fig.5. It is clearly indicated that when the bleed position is within the variable region of vortex pattern for example $\gamma=60^\circ \sim 120^\circ$, the side force control characteristics is effective. If it is in the invariable region such as $\gamma = 165^\circ$ or 180° , control behavior becomes ineffective. It is also shown from Fig.4 that there is different control efficiency from different bleed circumferential position. This simple and new active flow control technique to asymmetric vortices is flexible and we call it as single hole bleed perturbation active control technique.

4. CONCLUSIONS

Present experimental study of the effects of nose perturbations on the behaviors of asymmetric vortices over slender body models and its active control has been conducted at low speed wind tunnels with subcritical Reynolds number 1×10^5 at angle of attack 50° . Some conclusions can be obtained from this investigation.

1. There are four sensitive circumferential locations of manual perturbation at which bistable vortices over slender body are switched over by the micro-perturbation. And the C_y vs. γ curve appears two-cycle behavior.
2. The two-cycle behavior of C_y vs. γ curve for asymmetric vortices flow is gradually changed into one-cycle with increasing of microblowing rate at model nose tip as a manual perturbation to asymmetric vortices flow.
3. Based on above phenomena a single hole bleed perturbation active control technique is developed. For this new

technique the control characteristics is effective within a certain range of circumferential position of blowing perturbation.

ACKNOWLEDGEMENTS

This work was supported by National Natural Science Foundation of China (10172017) and Aeronautical Science Foundation (02A51048).

The ICAS 2004 CD Rom proceedings will have an ISBN number and an archive copy will be deposited in the National Library of Scotland.

REFERENCES

- [1] Malcolm G. Forebody Vortex Control. *Progress in Aerospace Sciences*, Vol.08, pp171-234, 1991
- [2] Malcolm G. Forebody Vortex Control –a progress review. AIAA-paper 93-3540-CP
- [3] Roos, F. W., Microblowing: An Effective, Efficient Method of Vortex-Asymmetry Management. AIAA 2000-4416. 2000
- [4] Rao D, Moskovitz C and Murri D., Forebody Vortex Management for Yaw Control at High Angles of Attack. *Journal of Aircraft*, Vol.24, No.4, pp248-254,1987
- [5] Ng T and Malcolm G. Forebody Vortex Control Using Small, rotatable strakes. *Journal of Aircraft*, Vol.29, No.4, pp671-678, 1992
- [6] Williams, D. R. A Review of Forebody Vortex Control Scenarios AIAA 97-1967, 1997
- [7] Bernhardt J. and Williams D. Proportional Control of Asymmetric Forebody Vortices. *AIAA Journal*, Vol.36, No.11, pp 2087-2093,1998
- [8] Bernhardt J. and Williams D. Close-loop control of forebody flow asymmetry. *Journal of Aircraft*, Vol.37, No.3, pp491-498, 2000
- [9] Deng X and Wang Y. Active control of Asymmetric vortices with bleed perturbation. *Proceedings of the Fourth International Conference on Fluid Mechanics*, Dalian, China, 2004
- [10] Hunt, B. L. Asymmetric Vortex Forces and Wakes on Slender Bodies. AIAA 82-1336, 1982
- [11] Deng Xueying and Wang Gang et.al. A Physical Model of Asymmetric Vortices Flow Structure in Regular State over Slender Body at High Angle of Attack, *Science in China* Vol.46, No.6, pp561-573, 2003
- [12] Chen Xuerui, Deng Xueying and Wang Yankui et al. Influence of nose perturbations on behaviors of asymmetric vortices over slender body. *ACTA MECHANICA SINICA*, Vol.18, No.6, pp581~592,2002

- [13] Keener E, Chapman G and Cohen L., etal. Side Force on a Tangent-ogive Forebody with a fineness Ratio of 3.5 at High Angles of Attack and Mach Number from 0.1 to 0.7. NASA TM X-3477, 1977
- [14] Roos F. and Magness C. Bluntness and Blowing for Flowfield Asymmetry Control on Slender forebodies. AIAA Paper 93-3409, 1993
- [15] Roos F. “Microblowing” for High-angle-of-attack Vortex Control on a Fighter Aircraft. AIAA Paper 96-0543, 1996

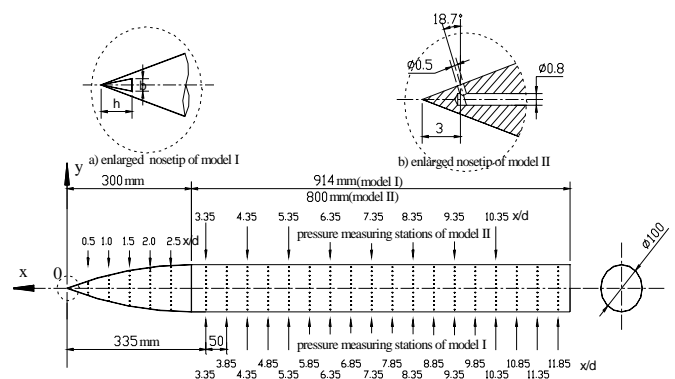


Fig.1 Sketch of test model

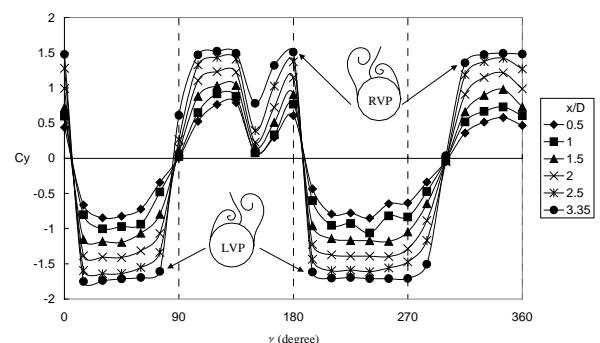
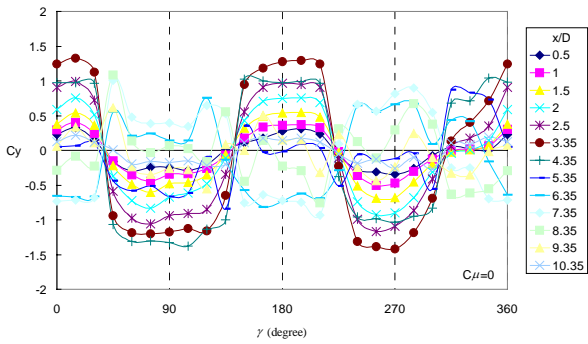
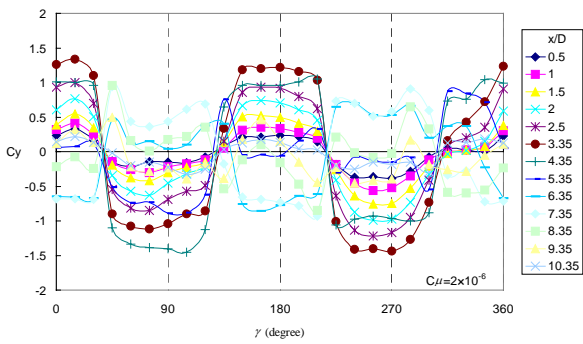


Fig.2 C_y - γ curves in the nose region of model ($\alpha=50^\circ$)



a) without bleed



b) with low blowing rate

Fig.3 Cy vs. γ of model ($\alpha=50^\circ$)

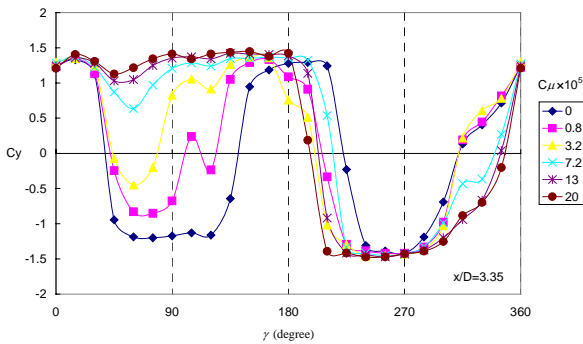


Fig.4 Variation of Cy vs. γ curves with blowing from model tests ($\alpha=50^\circ$)

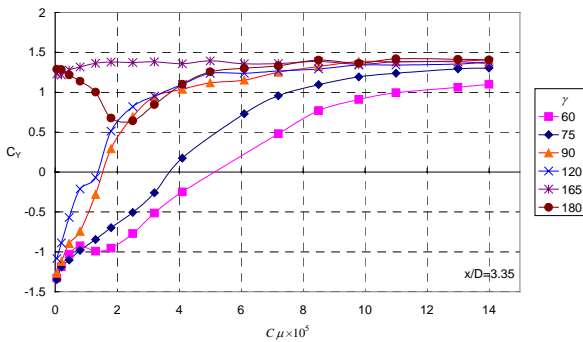


Fig.5 Cy vs. C_μ of model at different roll position ($\alpha=50^\circ$)